An improved solar wind electron-density model for pulsar timing

X. P. You[1,2,3], G. B. Hobbs[2], W. A. Coles[4], R. N. Manchester [2], J. L. Han[1]

ABSTRACT

Variations in the solar wind density introduce variable delays into pulsar timing observations. Current pulsar timing analysis programs only implement simple models of the solar wind, which not only limit the timing accuracy, but can also affect measurements of pulsar rotational, astrometric and orbital parameters. We describe a new model of the solar wind electron density content which uses observations from the Wilcox Solar Observatory of the solar magnetic field. We have implemented this model into the TEMPO2 pulsar timing package. We show that this model is more accurate than previous models and that these corrections are necessary for high precision pulsar timing applications.

Subject headings: pulsars: timing — sun: solar wind

1.   Introduction

It is now possible to make timing observations of millisecond pulsars to a precision of $\sim$100 ns. One of the most exciting applications of such data-sets is to search for the signatures of gravitational waves passing over the Earth. This is a major goal of the Parkes Pulsar Timing Array (PPTA) project (Hobbs 2005; Manchester 2006), which aims to observe 20 millisecond pulsars with a timing precision close to 100 ns over more than five years. Many phenomena can affect the pulse arrival times at this level of timing precision. A major contributor at our primary observing frequency of $\sim$1400 MHz is the interstellar and interplanetary medium (You et al. 2007). A small change in a pulsar's dispersion measure (DM; the integrated electron density along the line of sight to the pulsar) can cause significant

[1]National Astronomical Observatories, Chinese Academy of Sciences, Beijing 100012, China. Email:xpyou@ns.bao.ac.cn

[2]Australia Telescope National Facility, CSIRO, PO Box 76, Epping, NSW 1710, Australia

[3]Present address: School of Physics, Southwest University, Chongqing 400175, China

[4]Electrical and Computer Engineering, University of California at San Diego, La Jolla, California 92093, USA

time delays in the pulse arrival times. For example, at an observing frequency of 1400 MHz, a time delay of 100 ns is caused by a DM variation of only $\sim 5 \times 10^{-5}$ cm^{-3} pc. At this level, the solar wind effect is significant when the line of sight to the pulsar passes within $\sim$60° of the Sun.

The standard pulsar timing programs (TEMPO1[1] and TEMPO2; see Hobbs, Edwards & Manchester 2006, Edwards, Hobbs & Manchester 2006) calculate the solar contribution, DM$_\odot$, from a spherically symmetric model of the solar wind density which assumes a quadratic decrease with solar distance and ignores temporal variation:

$$\mathrm{DM}_\odot = 4.85 \times 10^{-6} \, n_0 \, \frac{\theta}{\sin\theta} \, \mathrm{cm}^{-3}\mathrm{pc}, \tag{1}$$

where n_0 is the electron density at 1 AU from the Sun (in cm^{-3}) and θ is the pulsar-Sun-observatory angle. By default, TEMPO2 chooses $n_0 = 4$ cm^{-3} whereas TEMPO1 uses $n_0 = 10$ cm^{-3}. However, the true electron density of the solar wind can change with longitude, latitude and time by a factor of at least four (McComas et al. 2000). You et al. (2007) demonstrated that this simple model is inadequate for PSR J1022+1001, a pulsar that lies close to the ecliptic plane.

There have been several previous analyses of the timing delays or DM variations due to the solar wind that occur in pulsar timing observations. For instance, the ecliptic latitude (β) of the Crab pulsar is only $-1.29°$. Lyne et al. (1988) showed, using a few observations within 5° of the Sun, that the maximum time delay due to the solar wind was about $500\,\mu$s at 610 MHz. Similarly, Phillips & Wolszczan (1991) showed that the DM changed by ~ 0.002 pc cm^{-3} when the line of sight to PSR B0950+08 ($\beta = -4.62°$) is close to the Sun. Cognard et al. (1996) observed PSR B1821$-$24 between the years 1989 and 1993 and showed that between December and January each year their timing residuals were significantly affected by the solar corona. More recently, Splaver et al. (2005) and Lommen et al. (2006) analysed data of PSRs J1713+0747 and J0030+0451 using the TEMPO1 model, but, instead of holding the electron density at 1 AU fixed, they fitted for this scaling factor. They obtained that $n_0 = 5 \pm 4$ cm^{-3} and $n_0 = 7 \pm 2$ cm^{-3} respectively.

Scherer et al. (1997) argued that the planetary companions to PSR B1257+12 (Wolszczan 1994) were artefacts of incorrectly modelling the solar wind. The closest planet to the pulsar produces a 25.3 d periodicity in the timing residuals which is remarkably close to periodicities seen in Pioneer 10 spacecraft data which are thought to be due to patterns in the solar wind caused by the Sun's rotation. Even though Wolszczan et al. (2000) proved that the periodicity was due to planetary companions (based on the use of the original TEMPO1

---

[1]http://www.atnf.csiro.au/research/pulsar/tempo

solar-wind model and multi-frequency observations) it is of interest to understand the effect of an unmodelled (or poorly modelled) solar wind on the measured pulsar parameters.

Recently, Ord et al. (2007) observed PSRs J1801−2304, J1757−2421, J1757−2223 and J1822−2256 when their lines of sight were close to the Sun. Their work has some overlap with ours as they also used observations from the Wilcox Solar Observatory and a model for the solar electron density. However, they concentrated on variations in pulsar rotation measures due to the solar magnetic field. In our work we model variations in pulsar dispersion measures and describe their implications for high precision pulsar timing.

In this paper we first describe a two-state solar wind model (§2) and our analysis technique (§3) before considering the implications for high precision pulsar timing (§4).

2. The two-state solar wind model

The solar wind is a complex system and important features are still poorly understood. A summary of the relevent physics can be found in Schwenn (2006). In brief, the solar wind can be thought of as having a quasi-static component which is bimodal and co-rotates with the Sun, and a transient component which has a time scale of hours to days. The best known of the transient events are coronal mass ejections, which typically cross any given line of sight about 5% of the time (Schwenn 1996). It is currently not feasible to model the complex transient events and we will concentrate on modeling the co-rotating wind structure, which has "fast" and "slow" components.

The slow wind has a relatively high density and apparently originates in or around active regions of closed magnetic geometry at low or middle latitudes. The fast wind has lower density and originates in regions with open magnetic field geometry called coronal holes. Large coronal holes are located over the solar poles during the years of minimum solar activity. Smaller and shorter-lived coronal holes occur at middle and low latitudes when solar activity is higher.

We note that original TEMPO1 model can be thought of assuming that the entire wind is a spherically symmetric slow wind, whereas the default TEMPO2 model assumes that the wind is entirely fast.

The electron density in the fast wind can be estimated from *Ulysses* and *SPARTAN* observations to give:

$$n_e = 1.155 \times 10^{11} R_\odot^{-2} + 32.3 \times 10^{11} R_\odot^{-4.39} + \tag{2}$$
$$3254 \times 10^{11} R_\odot^{-16.25} \ \ \mathrm{m}^{-3}$$

at a distance of $R_\odot$ solar radii (Guhathakurta & Fisher 1995, 1998).

We can approximate the electron density in the "slow wind" using a combination of the Muhleman & Anderson (1981) model fit to their own observations far from the Sun and the "Baumbach-Allen" model near to the Sun (Allen 1947),

$$n_e = 2.99 \times 10^{14} R_\odot^{-16} + 1.5 \times 10^{14} R_\odot^{-6} + \tag{3}$$
$$4.1 \times 10^{11} \left(R_\odot^{-2} + 5.74 R_\odot^{-2.7} \right) \ \text{m}^{-3}.$$

In order to determine $\text{DM}_\odot$ the electron density must be integrated along the line of sight to the pulsar. Information on whether a given position along the line of sight will be within the slow or the fast wind can be obtained from the Wilcox Solar Observatory[2] which provides daily maps of the solar magnetic field since May 1976. Following McComas et al. (2000), we assume that the slow wind occupies the zone within 20° of the magnetic neutral line and outside this is dominated by the fast wind and that both winds flow radially. To demonstrate our technique we show, in Figure 1, a synoptic chart showing the projection of the line of sight on to the Sun for PSR J1744−1134 on the 20th December 2004. As expected, this figure shows that some parts of the line of sight lie within the slow wind and some within the fast wind.

3. Data analysis and method

We use observations obtained for the Parkes Pulsar Timing Array (PPTA) project (Manchester 2006) to test our new model. A sample of 20 millisecond pulsars has been observed since February 2004 at intervals of 2-3 weeks at frequencies around 700 MHz, 1400 MHz and 3100 MHz. Details of the observations and the methods used to determine the DM variations are given by You et al. (2007).

For this paper we use data for four pulsars which have measurable DM variations due to the solar wind. PSRs J1022+1001 and J1730−2304 have ecliptic latitudes of −0.064° and 0.19° respectively and hence are eclipsed by the Sun each year. PSRs J1744−1134 and J1909−3744 have higher ecliptic latitudes (11° and −15° respectively) but can be timed with very high precision.

---

[2] `http://soi.stanford.edu/~{}wso/forms/prsyn.html`. To obtain data-sets suitable for TEMPO2 the CLASSICSS map should be selected with a LATITUDE projection. Full details can be obtained from the TEMPO2 on-line documentation (http://www.atnf.csiro.au/research/pulsar/tempo2).

We have implemented algorithms into TEMPO2 to integrate the electron density along a given line of sight assuming the fast- and slow-wind electron densities as given in Equations 2 and 3. For every observation, TEMPO2 calculates the projection of points along the line of sight to the pulsar on to the surface of the Sun, assuming the Carrington rotation rate and a mean wind velocity of $400\,\mathrm{km\,s^{-1}}$. These parameters are characteristic of the slow wind and are chosen since this component dominates both the wind dynamics and the dispersion contribution. Using data from the Wilcox Solar Observatory, TEMPO2 determines the position of the magnetic neutral line and, hence, the regions along the line of sight that are within the slow and fast winds. A numerical integration is then carried out to obtain the total electron column density of the solar wind along the line of sight and hence $\mathrm{DM}_\odot$. The derived values are not significantly dependent upon our assumptions about the wind rotation and velocity.

4. Results and Discussion

Tools are available within the TEMPO2 software to obtain such synopotic charts for any pulsar on any day since the start of the Wilcox Solar Observatory data in 1976. Figure 2 shows the DM variations according to our solar wind model for PSR J1744−1134 between the years 2004 and 2006. The predictions according to the earlier TEMPO1 and TEMPO2 models are also indicated in the Figure. We notice that the new model generally predicts DM values that are higher than the TEMPO2 model, but lower than the TEMPO1 model as expected from our two-state model. The new model is also not smooth. Variations of up to $\mathrm{DM}_\odot \sim 10^{-4}\,\mathrm{cm^{-3}pc}$ occur on a daily basis.

Differences between measured $\mathrm{DM}_\odot$ values (You et al. 2007) and the predictions using the original and new TEMPO2 models are shown in Figure 3 for the four pulsar datasets discussed in this paper. This figure shows that, for lines of sight that pass close to the Sun, the original TEMPO2 does not correctly predict $\mathrm{DM}_\odot$. However, the improved model predicts $\mathrm{DM}_\odot$ within experimental uncertainties for all observations.

Our data-sets are currently poorly sampled for lines of sight that pass close to the Sun. We have, therefore, compared our improved model predictions with observations of PSR B1821−24 using the Nançay radio telescope (Cognard et al. 1996). DM values were measured from their Figure 7. There appear to be significant non-solar variations in their measured DMs and we have removed a straight line fitted to the values more than $\sim 40\mathrm{R}_\odot$ from the Sun. Comparisons with the original TEMPO2 model and our improved model are shown in the right hand column of Figure 3. It is clear that the new model is a significant improvement over the previous TEMPO2 model. However, even with our improved model there
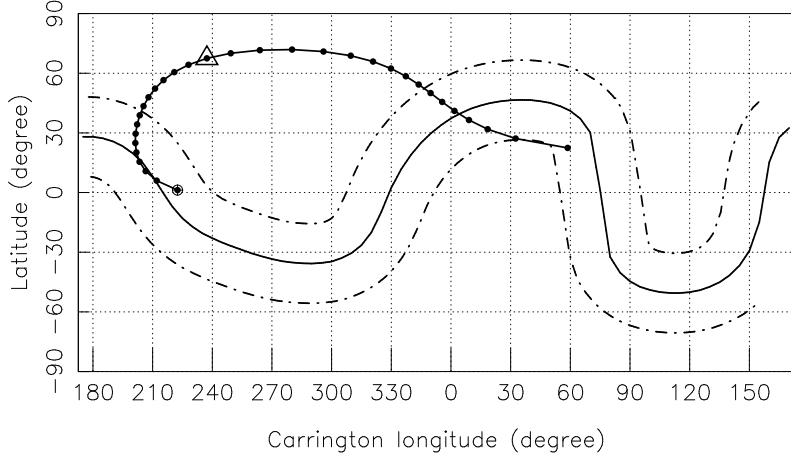
Fig. 1.— Projection on to the solar surface along wind streamlines of the line of sight to PSR J1744−1134 on 2004, December 20. The triangle shows the point of closest approach to the Sun and the open circle is the projected position of the Earth. Points are at 5° intervals in angle subtended at the Sun. The solid line indicates the position of the magnetic neutral line; the dashed lines on either side are plotted 20° away from the neutron line and delimit the region assumed to be dominated by the slow wind.
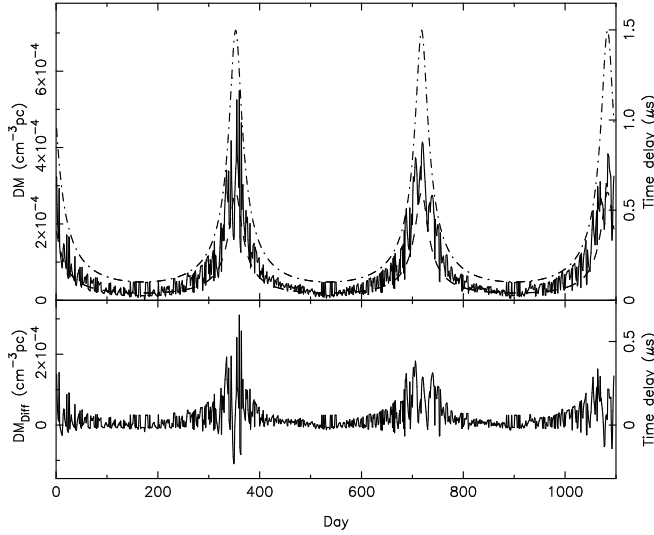

Fig. 2.— Solar-wind DM variations for PSR J1744−1134 from 2004 to 2006. The right-hand axis gives the corresponding time delay for an observing frequency of 1400 MHz. In the upper panel the solid line gives the DM variations from our new model. The dashed and dot-dashed lines indicate predictions of the original TEMPO2 model and the TEMPO1 models respectively. In the lower panel we plot the difference between the new model and the original TEMPO2 model.
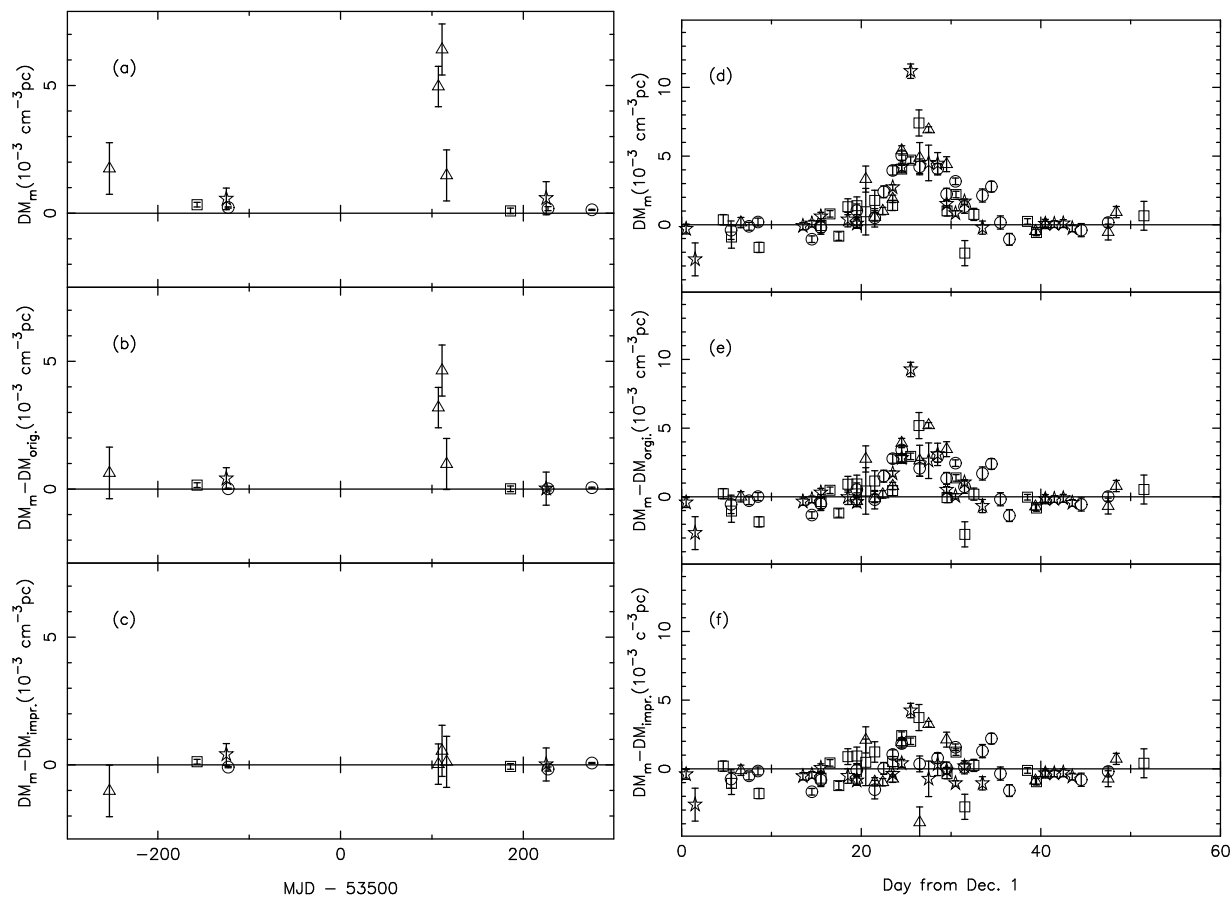
Fig. 3.— Left column: comparison of the measured DM values with the model predictions for PSRs J1022+1002 (triangle symbols), J1730−2304 (open stars), J1744−1134 (open squares) and J1909−3744 (open circles). Right column: comparison of the measured and predicted DMs for the Cognard et al. (1996) observations of PSR B1821−21. Triangle, star, square and circle symbols represent data starting in December 1989, 1990, 1991 and 1992, respectively. In both columns the upper panels gives the measured DM values without any solar wind correction. The middle panels give the difference between the actual values and those predicted using the original TEMPO2 model. The lowest panels show the difference between the measurements and the prediction using the improved solar wind model.

are some observations that are not consistent with our predictions. These inconsistencies occur at the closest approach of the line of sight to the Sun. At such close approaches our simple assumptions of the two-component wind model where the slow wind lies within 20° of the magnetic neutral line and radial wind flow with projection along mean flow streamlines may not be valid. We will be able to further test our model with future PPTA datasets having more precise and more closely sampled DM measurements at close angular distances to the Sun. Such results should help us to further improve the model.

4.1. Implications for high precision pulsar timing

Modern pulsar timing experiments are aiming to achieve rms timing precisions close to 100 ns over many years. At an observing frequency of 1.4 GHz the solar wind causes time delays of this magnitude for pulsars up to 60° from the Sun and significant deviations between the original and improved TEMPO2 models occur at $\lesssim 20°$ from the Sun.

In order to study the effect of an unmodelled, or poorly modelled, solar wind on pulsar timing parameters we used TEMPO2 to create simulated data-sets spanning three years for PSR J1744−1134. For these simulations we applied the improved solar-wind model and a specified amount of uncorrelated pulsar timing noise. We then either switched off all solar wind models or used the original TEMPO2 model before fitting for the pulsar's parameters. Deviations from the true values for various astrometric parameters are listed in Table 1. Clearly, the solar-wind model has a large effect on the values of the fitted parameters. For instance, for 100 ns rms timing residuals, the derived values for parallax and declination when using the standard TEMPO2 model deviate by $\sim 2.5\sigma$ and $\sim 11.0\sigma$ respectively from their true values. For any given pulsar, the error in each parameter will depend upon the rms timing residual, the data-span and the ecliptic latitude of the pulsar.

In order to test whether the solar wind can mimic planetary companions we have simulated a data-set for PSR B1257+12 with the same span and observing frequency as the Wolszczan (1994) observations. As we have no access to the original Wolszczan (1994) data-set, our simulated observations are uniformly sampled. A power spectrum of the solar wind contribution was computed with a rectangular window using the Lomb-Scargle algorithm. Since the data are uniformly sampled this is the same as the normal Fourier power spectrum. This spectrum, shown in the top panel of Figure 4, is dominated by harmonics of the annual modulation. To reduce the leakage of annual harmonics into the higher frequencies we removed the annual feature by subtracting a fit of a spherically symmetric model (Equation 1) to the residuals. The resulting spectrum is shown in the middle panel. There is no significant feature in either spectrum corresponding to the narrow 25.3-d peak seen in solar
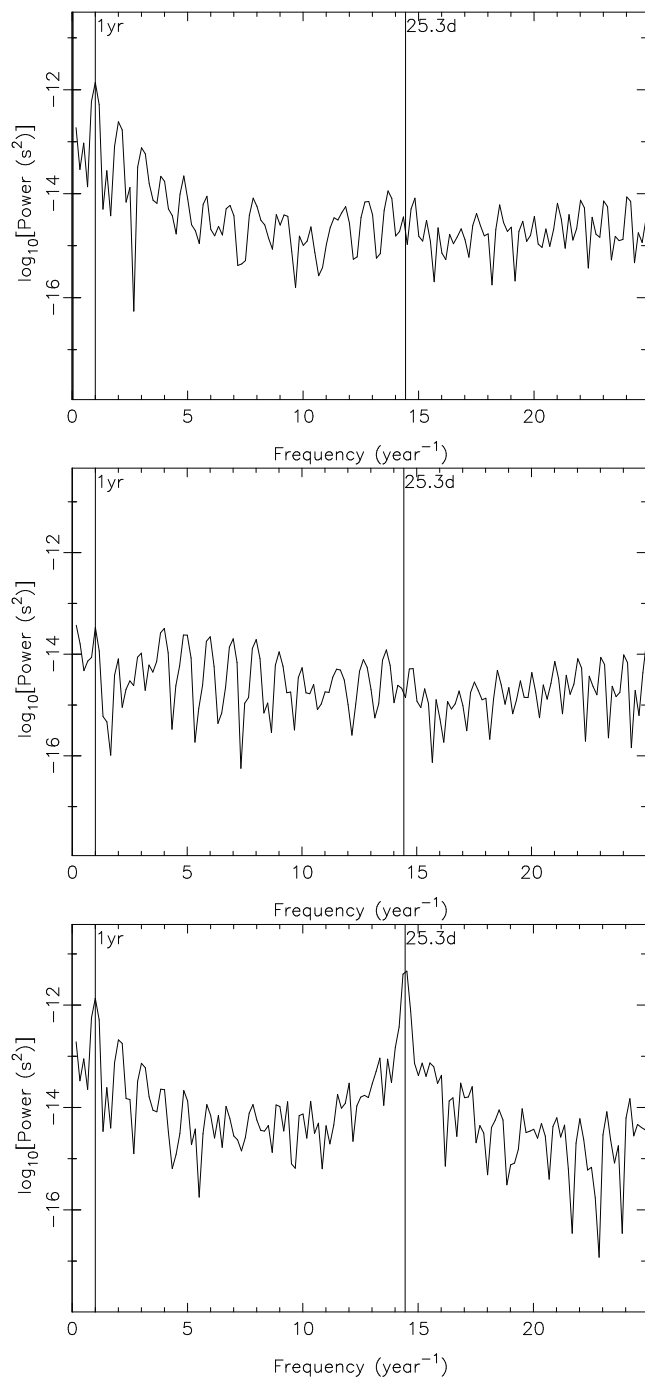
Fig. 4.— The upper panel shows the power spectrum of timing residuals contributed by the improved model of the solar wind for a simulated three-year data-span for the PSR B1257+12 system. In the middle panel we have reduced the power in the annual term and its harmonics by fitting the spherical wind model to the residuals and subtracting it. The bottom panel shows the power spectrum of residuals due to both the solar-wind model and the inner planet of the PSR B1257+12 system.

wind observations by Scherer et al. (1997). In fact we do not expect to see a sharp feature in the spectrum because the line of sight to the pulsar changes significantly during a solar rotation and the solar wind density itself evolves on that time scale. We have used TEMPO2 to introduce the expected signal from the planet and applied the same spectral analysis to the combined solar wind plus planet simulation. The resulting spectrum is plotted in the bottom panel. The contribution of the planet exceeds the solar wind noise by a factor of more than 100. Clearly Scherer et al. (1997) seriously overestimated the importance of solar noise in the detection of a planet around PSR B1257+12.

5. Conclusions

We have developed a new solar-wind model for pulsar timing experiments and shown that it gives a more accurate correction for delays due to the solar wind than earlier models. Use of the older solar-wind models (or no correction) leads to systematic errors in measured pulsar parameters. We have also shown that the solar wind cannot mimic the signal from inner-most planetary companion of PSR B1257+12 as suggested by Scherer et al. (1997). With the improved pulsar timing data expected in the future from projects such as the Parkes Pulsar Timing Array, use of the new model will make an important contribution to achieving the goals of these projects. The improved model has been implemented in the TEMPO2 software package and we recommend that it be used for all high-precision timing applications.

REFERENCES

Allen, C. W. 1947, MNRAS, 107, 426

Cognard, I., Bourgois, G., Lestrade, J.-F., Biraud, F., Aubry, D., Darchy, B., & Drouhin, J.-P. 1996, A&A, 311, 179

Edwards, R. T., Hobbs, G. B., & Manchester, R. N. 2006, MNRAS, 372, 1549

Guhathakurta, M. & Fisher, R. 1998, ApJ, 499, L215

Guhathakurta, M. & Fisher, R. R. 1995, Geophys. Res. Lett., 22, 1841

Hobbs, G. 2005, PASA, 22, 179

Hobbs, G. B., Edwards, R. T., & Manchester, R. N. 2006, MNRAS, 369, 655

Lommen, A. N., Kipphorn, R. A., Nice, D. J., Splaver, E. M., Stairs, I. H., & Backer, D. C. 2006, ApJ, 642, 1012

Lyne, A. G., Pritchard, R. S., & Smith, F. G. 1988, MNRAS, 233, 667

Manchester, R. N. 2006, Chin. J. Astron. Astrophys., Suppl. 2, 6, 139

McComas, D. J., Barraclough, B. L., Funsten, Gosling, J. T., Santiago-Muñoz, E., Skoug, R. M., Goldstein, B. E., Neugebauer, M., Riley, P., & Balogh, A. 2000, J. Geophys. Res., 105, 10419

Muhleman, D. O. & Anderson, J. D. 1981, ApJ, 247, 1093

Ord, S. M., Johnston, S., & Sarkissian, J. 2007, ArXiv e-prints, 705

Phillips, J. A. & Wolszczan, A. 1991, ApJ, 382, L27

Scherer, K., Fichtner, H., Anderson, J. D., & Lau, E. L. 1997, Science, 278, 1919

Schwenn, R. 1996, Ap&SS, 243, 187

—. 2006, Living Reviews in Solar Physics, 3, 2

Splaver, E. M., Nice, D. J., Stairs, I. H., Lommen, A. N., & Backer, D. C. 2005, ApJ, 620, 405

Wolszczan, A. 1994, Science, 264, 538

Wolszczan, A., Hoffman, I. M., Konacki, M., Anderson, S. B., & Xilouris, K. M. 2000, ApJ, 540, L41

You, X. P., Hobbs, G., Coles, W. A., Manchester, R. N., Edwards, R., Bailes, M., Sarkissian, J., Verbiest, J. P. W., van Straten, W., Hotan, A., Ord, S., Jenet, F., Bhat, N. D. R., & Teoh, A. 2007, MNRAS, 378, 493

Table 1: Effect on timing parameters for different rms timing residuals when comparing the new solar wind model to 1) no model and 2) the original TEMPO2 model.

Rms resid. (μs)	Parameter	No model (σ)	Orig.T2 model (σ)
0.0	Right ascension	11.8	9.0
	Declination	52.1	22.2
	Parallax	26.6	4.1
0.1	Right ascension	5.9	2.7
	Declination	33.4	11.0
	Parallax	17.6	2.5
1.0	Right ascension	1.3	1.7
	Declination	3.8	0.8
	Parallax	2.7	0.7